Title: **Integrated AFP Manufacturing and Stress Analysis/Design Process**

Authors: August Noevere, Craig Collier

ABSTRACT

Design of structures manufactured with automated fiber placement machines presents a unique set of challenges when compared to traditional hand layups. However, it has a significant advantage in simulation of the manufacturing process. Fiber is placed by a robot, providing an accurate digital model of the manufactured part. In this paper, a process is presented to map this manufacturing data from Vericut Composite Programming (VCP) to the stress analysis performed in HyperSizer. Such a process makes it possible to incorporate manufacturing constraints in the design process, thereby streamlining the laminate design and potentially reducing the weight of the structure.

INTRODUCTION

Use of Automated Fiber Placement (AFP) has become increasingly popular in recent years due to its ability to create ply layups far more consistently and quickly than traditional hand-layup approaches, especially for large structures. However, use of AFP manufacturing presents a new set of challenges in the design process. In particular, this paper addresses the impact of fiber angle deviation and tow overlaps (laps) and gaps on the overall design and stress analysis process. Both of these features are closely related to the tow paths generated by Path Simulation Software (PSS) for manufacturing. Thus, iteration is required between the manufacturing and stress analysis disciplines to achieve a satisfactory laminate design. This paper presents a streamlined design process for rapid iteration between the HyperSizer (stress analysis) and VCP (PSS) software to achieve this objective.

Description of Analysis Approach

The first challenge addressed here is fiber angle deviation, which appears in two different forms. One way that fiber angle deviation is tracked is the deviation that occurs

August T. Noevere, Craig S. Collier, Collier Research Corporation, 760 Pilot House Drive, Newport News, VA 23662, U.S.A..

from fiber directions that are assumed in the Finite Element Model (FEM). When the FEM is first created, fiber directions are usually assumed because the actual as-manufactured directions are not yet fully understood. Thus, when the stress analyst first generates ply counts, the strength and stability Margins of Safety (MS) are based on these assumed directions. After AFP tow paths have been generated, there is usually some deviation between the assumed directions and the as-manufactured directions (on a complex curvature part). These deviations can potentially cause negative MS, requiring the initial laminate design to be revisited.

The second form of fiber angle deviation to be considered is through-thickness deviation, or how far the laminate deviates from nominal 0/45/90 orientations. In the current state of certification requirements for aerospace structures, it is generally preferred that laminates stay as close as possible to these orientations. The challenge with through-thickness deviation is that it can vary over the surface of a complex-curvature part. Rotating a ply to improve the deviation in one area may worsen the deviation in another. Thus, it is necessary to track this deviation each time a change is made to tow paths.

Another challenge to be addressed is the occurrence of laps and gaps. These features are often found where paths converge or diverge and adjacent tows must be cut to accommodate each other. The laps and gaps essentially cause extra or missing material in a ply, which results in an overall thickness deviation of the laminate, which can impact strength margins, especially if these features stack on each other. Overall stiffness of the structure can be impacted as well if there are significant accumulations of features in one place.

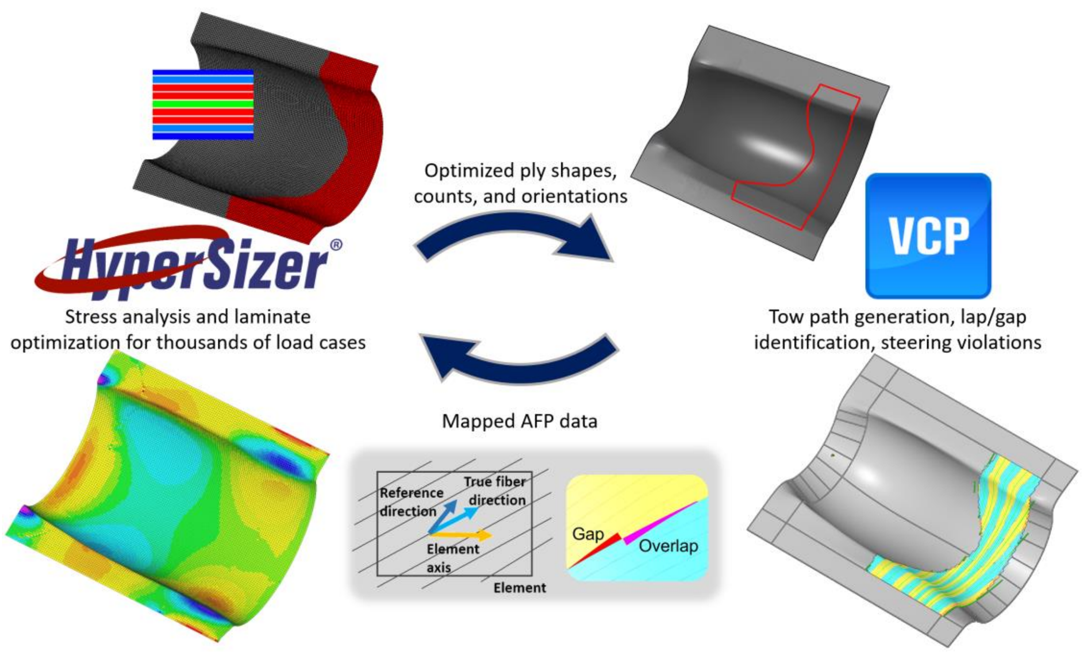

Figure 1. Flow chart for stress analysis, ply design, and analysis update process.

To address the challenges described above, a process was created to map fiber directions and lap/gap geometry from VCP to the FEM mesh in HyperSizer. This allows the stress analysis to be re-run to capture any changes in strength margins due to tow path adjustments made in VCP. Additionally, any changes to ply counts and ply boundaries made by HyperSizer can be quickly mapped to VCP for generation of new tow paths. This process is shown in the flow chart in Figure 1.

A generic Inner Fixed Structure (IFS), commonly found in high-bypass turbofan engines on commercial airliners, was used to demonstrate the AFP design and analysis process presented in this paper. The IFS is located behind the fan of the engine, usually underneath the thrust reversers. Location of the IFS is indicated in Figure 2.

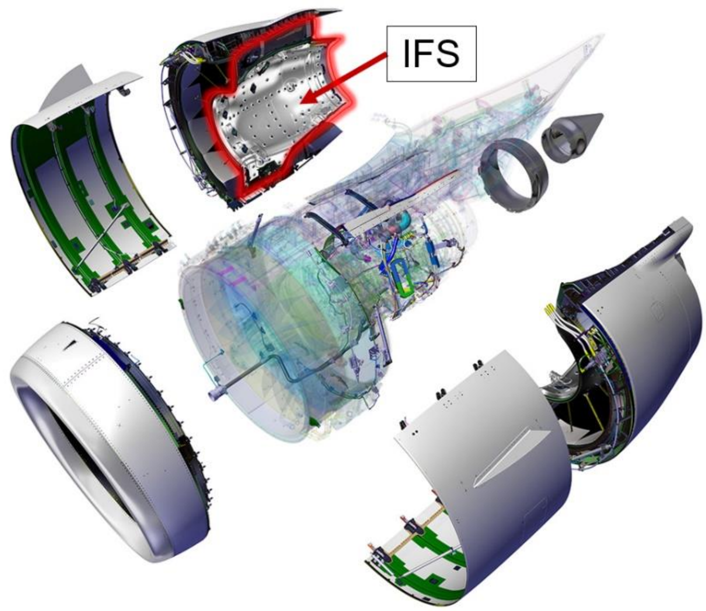

Figure 2. Location of IFS in engine.

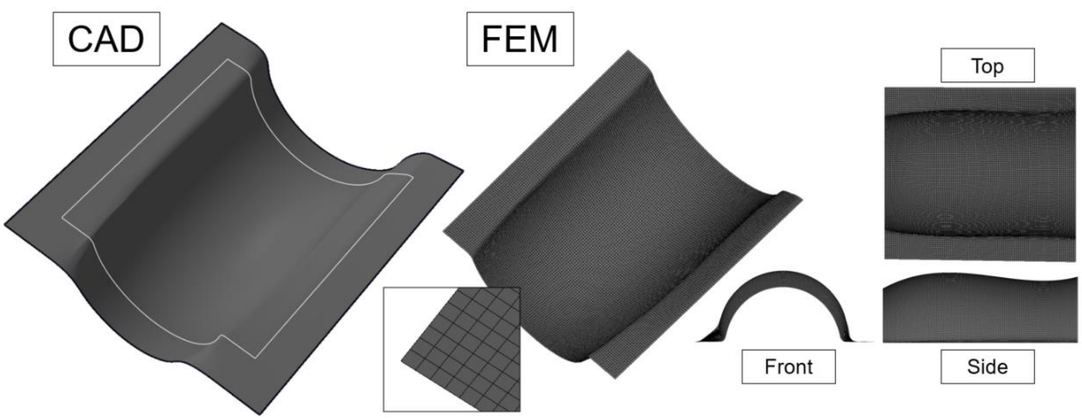

Figure 3. CAD and FEM for IFS structure.

Description of Model

The IFS is usually sized for both strength and acoustic requirements. In this presented design process, the acoustic requirements are neglected for simplicity. A Computer Aided Drafting (CAD) model and corresponding FEM were created for the IFS, as shown in Figure 3. Note that the boundary of the CAD model extends beyond that of the FEM, which is necessary to represent the layup tool surface.

The FEM contains a structured mesh of 16874 quadrilateral elements. Mesh density was selected so that the element size is roughly equal to the AFP tape width (0.5”). Three load cases were applied to the model, cruise, +2.5g maneuver, and a -1.0g maneuver.

INITIAL LAMINATE/PLY DESIGN

The IFS was sized as a composite sandwich concept, consisting of two facesheets (symmetric to each other) and an aluminum honeycomb core. The first step of the sizing process was to determine optimum shapes for the sizing zones of the structure. Next, laminates were generated within each zone to satisfy strength requirements. The final step was to perform laminate sequencing between the zones to generate final plies for the top and bottom facesheets of the structure.

Zone Shape Optimization

Some structures, such as aircraft fuselage skins, often have zone shapes restricted by placement of frames and stiffeners on the skin. The IFS, however, is less restricted and can have ply drops with more “organic” shapes to follow internal loads in a more optimum manner. The use of AFP manufacturing further facilitates these organic ply shapes because the plies are placed by a machine, rather than being cut and placed by hand. Thus, large and irregular plies are more feasible to manufacture.

Considering the above, HyperSizer Express [1] was used to define optimum sizing zones for the IFS. This tool performs a per-element optimization to generate optimum zone shapes. The typical starting point used in Express is a “boilerplate” design, consisting of a uniform thickness plate on the entire structure. The intention is to have an un-biased starting point for the load path in the structure. HyperSizer Express then enters an FEA iteration cycle where it generates a potentially unique laminate for every element in the structure. During this process, similarity and proximity of elements are analyzed to determine which elements should be grouped together into sizing zones. The user is ultimately able to select a zone density, to bring manufacturing complexity into the picture. Zone density/complexity is directly tied to weight of the structure. Fewer zones ultimately drive the weight of the structure up. Figure 4 shows an example of the two extremes, as well as the selected zone configuration.

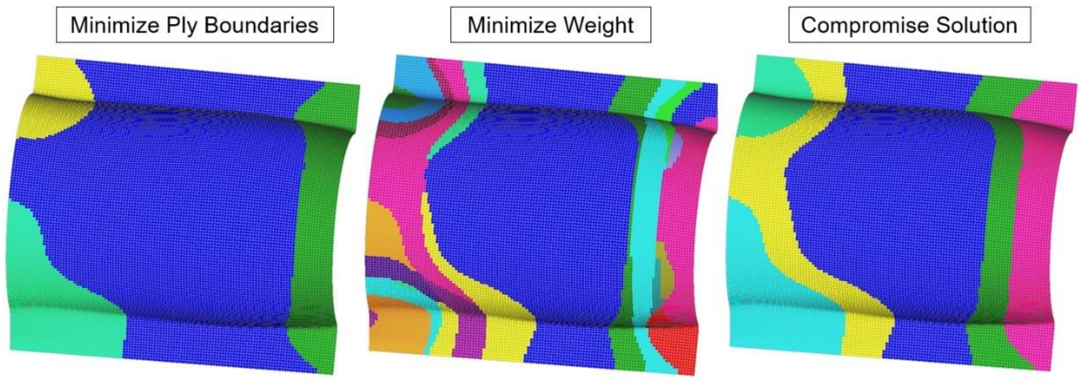

Figure 4. Zone shape optimization solutions.

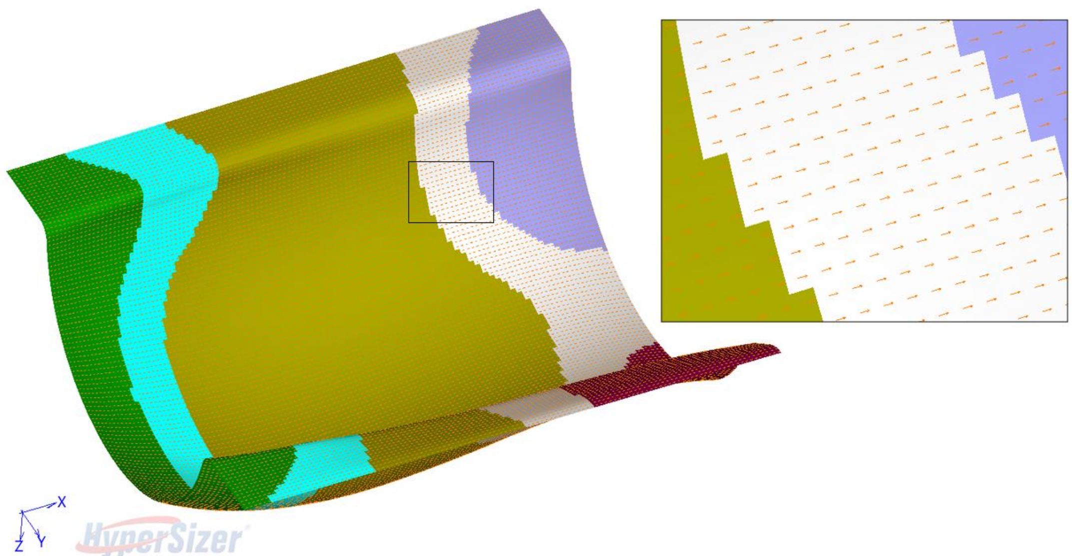

Figure 5. Reference fiber direction on elements.

Laminate Sizing and Sequencing

After zone shapes were optimized, HyperSizer was used to generate optimum laminates for each zone. These laminates were generated considering the loads described previously and a variety of failure criteria. These criteria included ply-based max strain and stress criteria, as well as Tsai-Wu [2], Tsai-Hill [3], and Hoffman interaction criteria. Additionally, because the structure has a honeycomb core, criteria such as facesheet wrinkling, intercell dimpling, core shear, core crush, and core crimping were included in the sizing. To simplify the sizing process, the core was sized to a uniform thickness of 0.75” and a density of 6.1 pcf. Alternatively, HyperSizer is capable of sizing the core independently in each zone (both core thickness and material).

Note that for this step of the sizing process, HyperSizer performs laminate analysis with fibers oriented in “reference” directions. For structures with complex curvature, the as-manufactured fiber directions are dictated by the curvature of the tool. However, at this point in the sizing process, the as-manufactured fiber directions are unknown. Thus, a “reference” direction for 0° fibers was assumed to align with the global x-axis of the structure. Fibers in the 45° and 90° direction are aligned accordingly. The reference direction for 0° fibers is shown in Figure 5.

During the laminate sizing process, HyperSizer generates many feasible laminates for each zone instead of just a single laminate. The laminates for each zone typically have similar total thickness (and thus weight) but contain a variety of different ply percentages (for each orientation) and different stacking sequences. This pool of laminates allows HyperSizer to perform a final laminate sequencing. In the sequencing step, plies from laminates in each sizing zone are connected to form "global" plies that span multiple zones. HyperSizer sorts through a large number of possible sequencing solutions while trading manufacturability against mass, with a user-defined weighting for either trait. Some of the final global plies from the sequencing process are shown in Figure 6. In all, 22 unique plies were defined for the IFS. Ply counts for each sizing zone are shown in Figure 7.

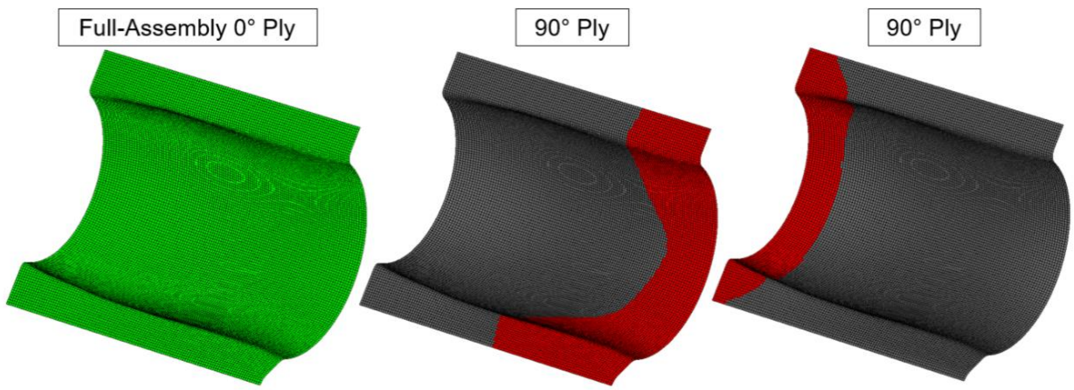

Figure 6. Example ply shapes.

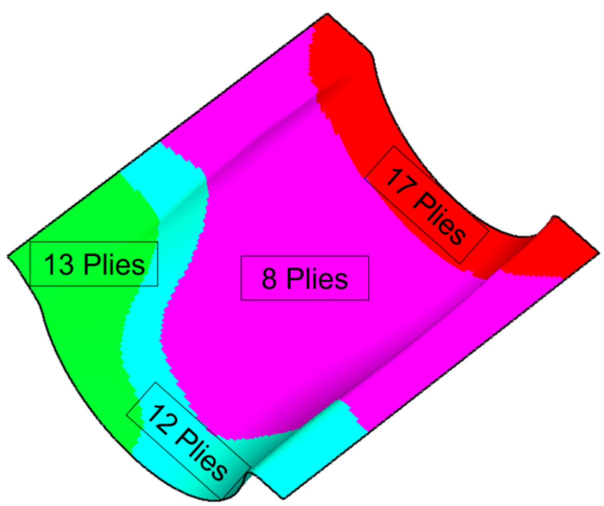

Figure 7. Ply counts for each sizing zone.

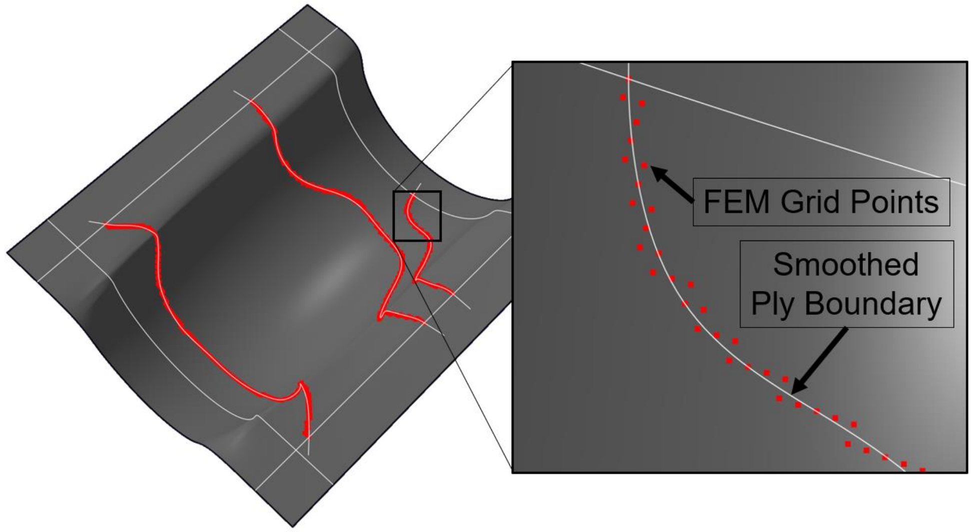

Figure 8. Transfer of FEM ply boundaries to CAD.

Transfer of Plies to CAD

Once plies had been defined in HyperSizer, it was necessary to translate them from a FEM-based format to a CAD-based format. HyperSizer is a FEM-based tool; as a result, the zone/ply boundaries optimized by HyperSizer are represented by a series of grid points along the edges of FEM elements. This format is not suitable for final CAD plies due to the jagged shape caused by the element boundaries. To address this issue, the element-based ply boundaries were exported and passed to CATIA [4] using a macro. In addition to simply passing the XYZ points to CATIA, the macro automatically generated smoothed curves for each of the ply boundaries. These features are shown in Figure 8. Once these curves were generated for the ply boundaries, the CAD-based ply definitions were produced to match the definitions in HyperSizer.

Generation of Tow Paths for AFP

The final step of the initial design process was to generate AFP tow paths to fill in the ply boundaries previously defined. The ply definitions from CATIA were exported to VCP for this purpose. During generation of paths there are several manufacturing considerations made that are closely tied to strength analysis of the structure, as discussed in subsequent sections. For a structure with significant curvature, such as the IFS, the as-manufactured fiber directions and lap/gap placement depend on manufacturing parameters specified in VCP.

Tape width has a significant impact on as-manufactured fiber directions because it dictates how much the tows can be steered as they are being placed. Narrow tape can be steered to a tighter radius without causing AFP defects such as tow puckering and wrinkling. This makes it possible to minimize fiber angle deviation on complex curvature. However, utilizing a narrow tape typically produces more laps and gaps simply because there are more tows and it also increases manufacturing time because more passes of the AFP machine are needed. For the IFS structure, a tape width of 0.5” was used with a corresponding steering radius limit of 300”.

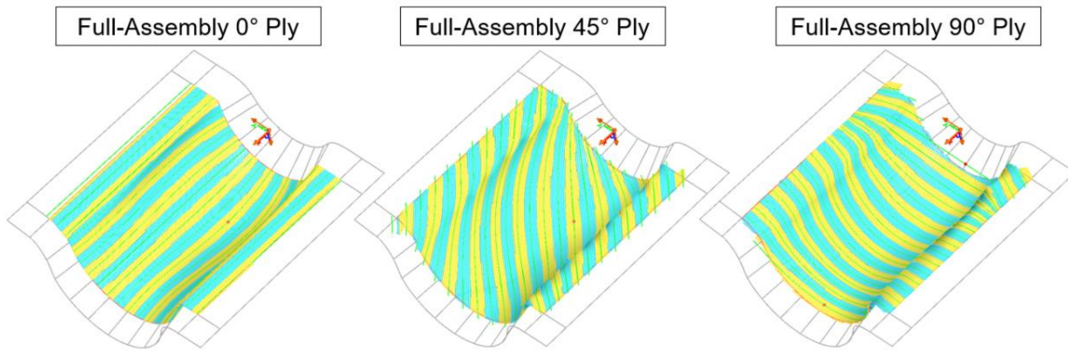

Figure 9. Example tow paths for the IFS.

In addition to tape width, layup strategy also has a significant impact on fiber direction and tow laps/gaps. The layup strategy dictates which path generation algorithm VCP uses when generating tow paths. The two extremes are "rosette" paths and "natural" paths. The rosette paths produce fiber directions that are ideal from a certification perspective: they will always have perfect 0/45/90 orientations through-thickness at any location in the part. However, the amount of fiber steering needed to achieve rosette paths on complex curvature often violates the steering limit of the tape, resulting in AFP defects. The other extreme are natural paths, which follow the natural curvature of the structure, and thus typically have minimal AFP defects. However, these paths tend to have greater fiber angle deviation. There are also a variety of other layup strategies to generate paths that are a compromise between rosette and natural paths.

For the IFS structure, natural paths were selected for the layup strategy due to the significant curvature in the structure, as well as to demonstrate the non-traditional laminate mapping and analysis capability described in the next section. An example of tow paths for 0°, 45°, and 90° plies is shown in Figure 9.

MAPPING AFP FIBER DIRECTIONS

The first of the key AFP laminate strength analysis technology presented in this paper is the ability to map and analyze as-manufactured fiber directions from the path simulation software to HyperSizer. This process enables migration away from traditional 0/45/90 laminates by providing a streamlined approach to analyze each unique laminate stack across the entire structure. For a complex curvature part, each ply will have varying amounts of deviation across the structure. This causes a unique combination of fiber angles at almost every location in the structure. By mapping fiber directions from VCP to the FEM in HyperSizer, these unique fiber angles can be analyzed at every point. The mapping is achieved by passing the locations of FEM element centroids to VCP, which in turn provides a unit vector corresponding to fiber orientation at each element. This process is shown in Figure 10.

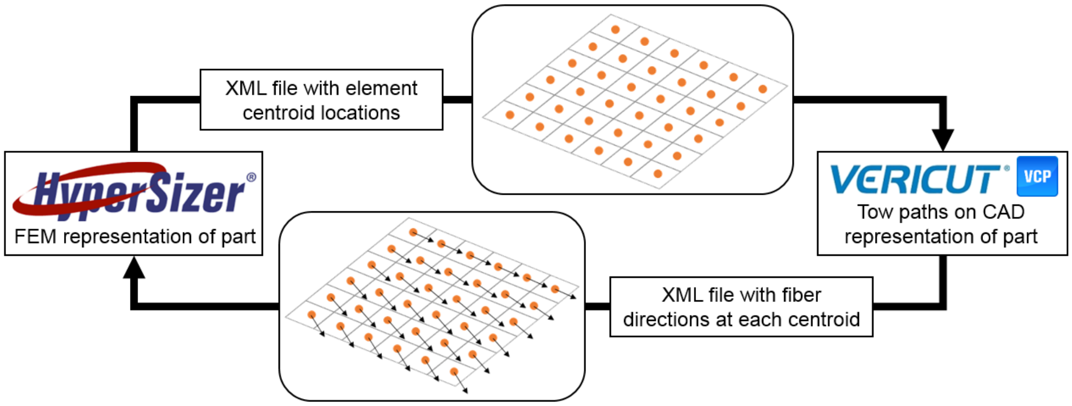

Figure 10. Fiber direction mapping process. [5]

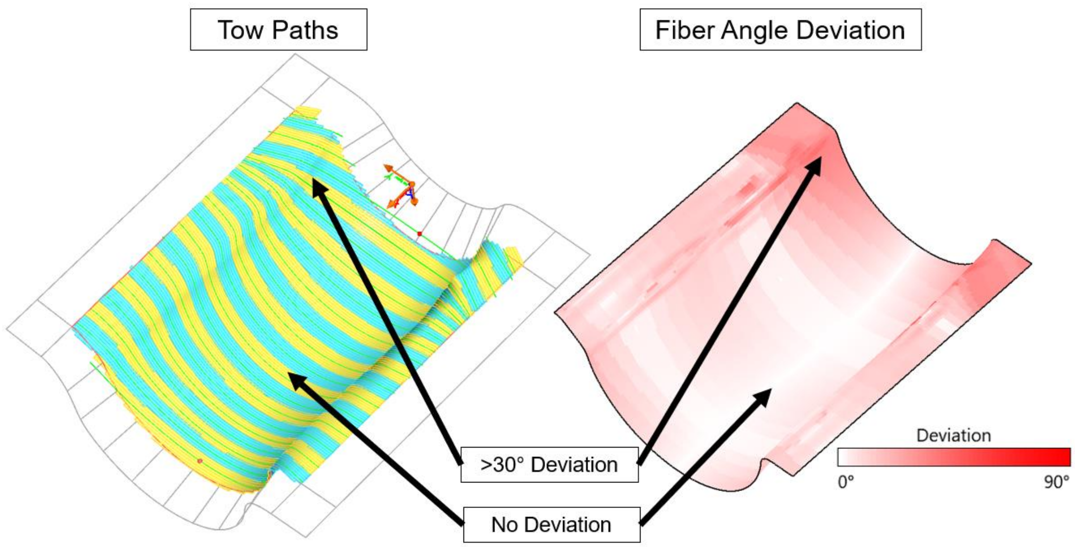

Figure 11. Fiber angle deviation for 90° ply.

Fiber Angle Deviation

There are two forms of fiber angle deviation that are important to consider. The first is deviation from the rosette fiber directions. As discussed previously, the rosette fiber direction is derived from alignment with a single global axis and the element normal. This direction is typically assumed for the initial laminate sizing and analysis, due to lack of better information. Thus, when the as-manufactured fiber directions are mapped it is important to measure the deviation of each ply from the rosette direction used in the initial analysis. Significant deviation can be found on the IFS where the structure has a decreasing radius. For 90° plies in particular, this region forces tow paths to tip away from the hoop direction, as shown in Figure 11.

The second form of deviation considered is calculated at the laminate level, as opposed to the previous per-ply calculation. This is the through-thickness deviation over the laminate. Because the deviation of each tow path varies over the structure, the through-thickness deviation at any given location on the structure is potentially unique. The through-thickness deviation is determined by calculating a new reference coordinate system for each element. For example, consider a laminate with two plies that end up as a [5/55] laminate with AFP tow paths with respect to the rosette, or reference coordinate system. These plies would have a deviation of +5° and +10°. However, since *local* through-thickness deviation is the metric of interest, a new reference direction could be calculated to be located at +7.5° from the original. This new reference direction gives a deviation of -2.5° and +2.5° for the two plies. This logic can be applied to a laminate with any number of plies with the following equation.

$$\theta_{new\,ref,i} = \frac{\theta_{dev,min,i} + \theta_{dev,max,i}}{2} \quad (1)$$

The new reference orientation for the i^{th} element ($\theta_{new\,ref,i}$) can be calculated from the min and max deviation of *any* ply in that element ($\theta_{dev,min,i}$ and $\theta_{dev,max,i}$). Note that these deviations must be adjusted to fall within 22.5°. This is because maximum absolute deviation for 0/45/90 plies can never be greater than 22.5° (= 45°/2). This approach was used to generate the through-thickness deviations plotted in in Figure 12.

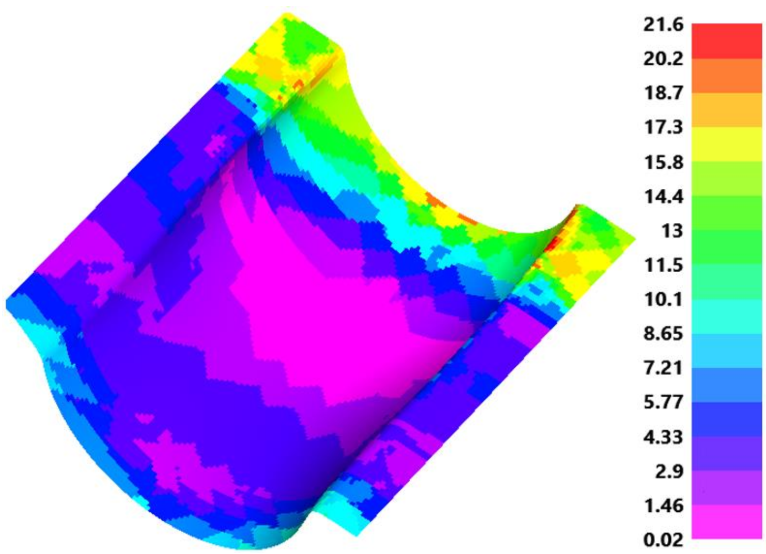

Figure 12. Through-thickness fiber angle deviation (degrees).

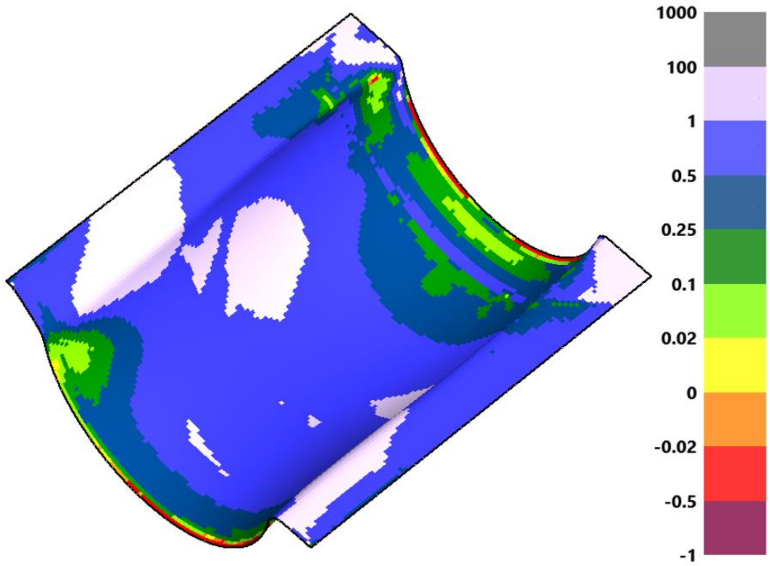

Figure 13. Margins from analysis with updated fiber directions.

Strength Margin Assessment

After the fiber directions were mapped to the FEM in HyperSizer, they were also included in an updated strength margin assessment. For this analysis, HyperSizer evaluated the ply-based strength margins using the unique fiber angles found in each element, instead of the 0/45/90 angles as defined in the original analysis. This approach is permissible in a Classical Lamination Theory (CLT) analysis, which allows ply angles of any continuous value. Note that this does require rotating the load in each element corresponding to the updated local reference coordinate system.

Figure 13 shows the margins after running the updated strength analysis. The plot shows a reduction in margins compared to the original analysis, especially around the two curved openings at either end of the structure. This result lines up with the fiber angle deviations observed above. The original laminate was sized to have a margin close to zero, so any deviation of the fibers can easily cause the margin to become negative.

FEM Update with AFP Fiber Directions

To improve the accuracy of the margins reported above, it is necessary to update the FEM and rerun FEA to get new element loads. The fiber angle deviations change the stiffness of the structure, and thus change the load distribution. To update the FEM, a unique laminate property card (PCOMP in Nastran) is generated for each element. This is necessary to capture the varying fiber angles over the entire structure. Strength margins corresponding to the updated FEA loads are shown in Figure 14.

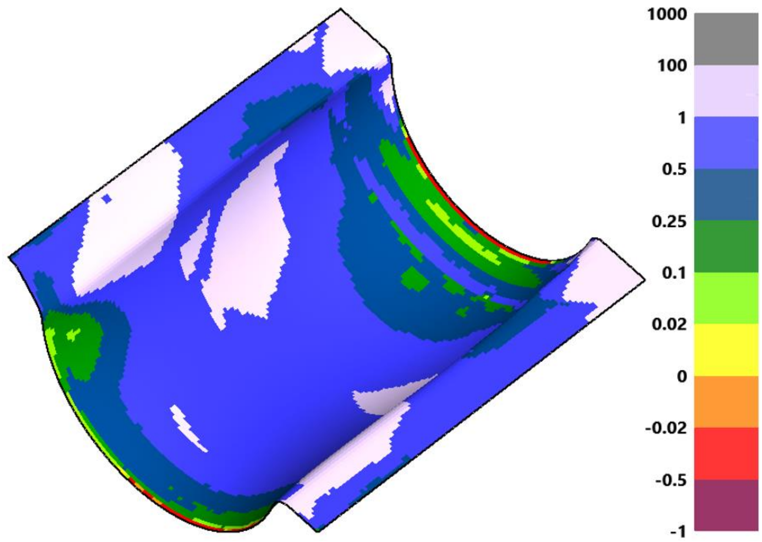

Figure 14. Margins with updated fiber directions and FEA iteration.

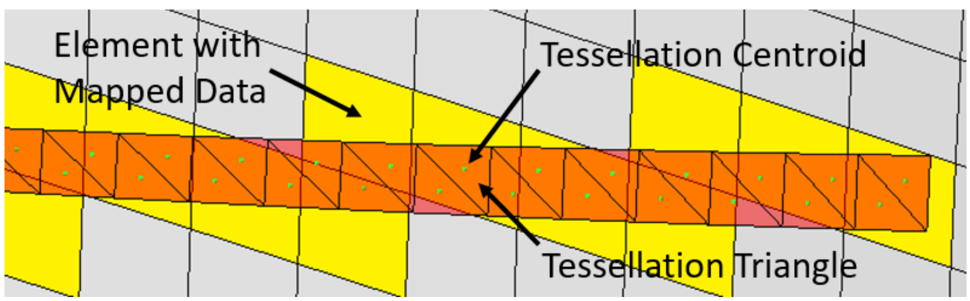

Figure 15. Mapping of tessellated lap/gap feature to FEM mesh.

MAPPING LAPS AND GAPS

Laps and gaps are another AFP feature that can have a significant impact on the strength of the structure. The size and shape of laps and gaps are defined by several different parameters. Primarily, these features are caused where tow paths converge or diverge; a higher rate of convergence or divergence will cause short, triangular laps and gaps, whereas a low rate of path convergence will cause long and slender laps and gaps. Convergence of the paths depends on both the curvature of the surface as well as user-defined parameters for the path generation (layup strategy, start point, etc.). Additionally, width of the tape impacts lap and gap geometry. Wider tape will cause fewer laps and gaps overall, but those features will be larger than found with narrower tape.

The methodology used to map the laps and gaps from VCP to HyperSizer is described in detail in Reference [5]. The mapping process first performs a tessellation of the lap and gap features. The centroid of each tessellation element is then projected onto the FEM to determine which FEM element is adjacent to the feature. This is repeated until all lap and gap features have been placed on the FEM. An example of this mapping is shown in Figure 15.

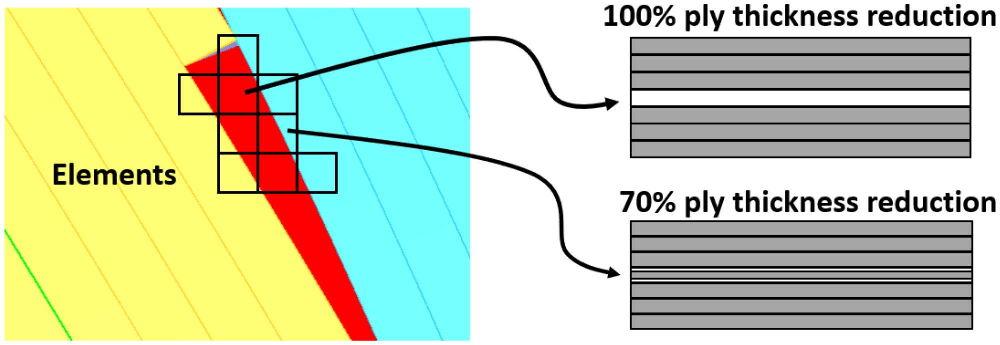

Figure 16. Ply thickness scaling approach.

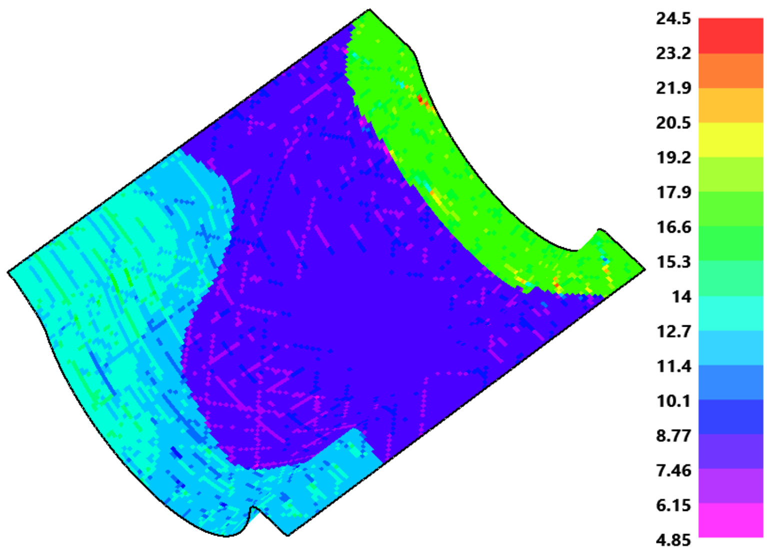

Figure 17. Accumulated thickness of laps and gaps (ply count plotted).

One challenge presented by this mapping process is how to translate the continuous geometry of laps and gaps to the discrete mesh of the FEM. The approach taken was to scale ply thickness down according to how much of an element it covers. For example, if a gap covers 100% of an element's area, the thickness of that ply will be scaled to zero in both the laminate thickness calculation and laminate analysis (presented next). This approach is depicted in Figure 16.

Laminate Thickness Deviation

Because laps and gaps tend to appear in areas with significant curvature, the laps and gaps from multiple plies often accumulate and can result in significant thickness deviation from the nominal laminate. This can be a concern for portions of the structure that must interface with other structures, such as a bonded or bolted interface.

After laps and gaps were mapped to the IFS FEM with the methodology described previously, it was possible to track how they accumulated through the thickness of the laminate. In each element, the thickness adjustments for laps and gaps are simply summed up to determine total laminate thickness for that element. The thickness of the laminate for the i^{th} element (t_i) is calculated from the equation below. The ratio R describes the fraction of element area that is covered by a lap or gap feature.

$$t_i = \sum_{j=1}^{n_{ply}} \left(1 + R_{laps}(i,j) - R_{gaps}(i,j)\right) \cdot t_{ply} \tag{2}$$

Figure 17 shows a plot of total laminate thickness on the IFS, determined from the calculation described above. Note that some of the more extreme deviations on this plot would likely be partially flattened down by the roller on the AFP machine during manufacturing. The displayed thickness accumulations could also be improved by regenerating tow paths with more staggering for plies of similar orientation. If tow paths of the same orientation are generated using the same starting point, the laps and gaps tend to accumulate in the same location. Staggering starting points of the plies can help alleviate this issue.

Strength Margin Assessment

The ply thickness scaling described previously for the lap/gap mapping also applies to the approach taken for the lap/gap strength analysis. In the CLT analysis performed by HyperSizer, the individual ply thicknesses are scaled according to the presence of laps or gaps in each element. A plot of this updated margin assessment is shown in Figure 18. The presence of laps and gaps in the analysis is made apparent by the strips of lower (and in some cases, negative) margins. Note that these margins include the fiber angle deviations presented in the previous section.

FEM Update with AFP Laps and Gaps

As with fiber angle deviation, it is necessary to update the FEM and rerun FEA to capture the redistribution of material in the structure. The laps and gaps have an impact on the load distribution because they alter the stiffness of each element. Elements with more gaps will be thinner and shed load into surrounding elements. Conversely, elements with more laps will be thicker and thus pick up more load. As a result, lap/gap analysis performed with without a FEM update is often conservative.

The strength margins produced after the FEM update with laps and gaps are shown in Figure 19. This plot shows that the vast majority of negative margins due to laps and gaps were resolved by obtaining the updated load distribution. The only negative margins that remain are those caused by fiber angle deviations, discussed in the previous section.

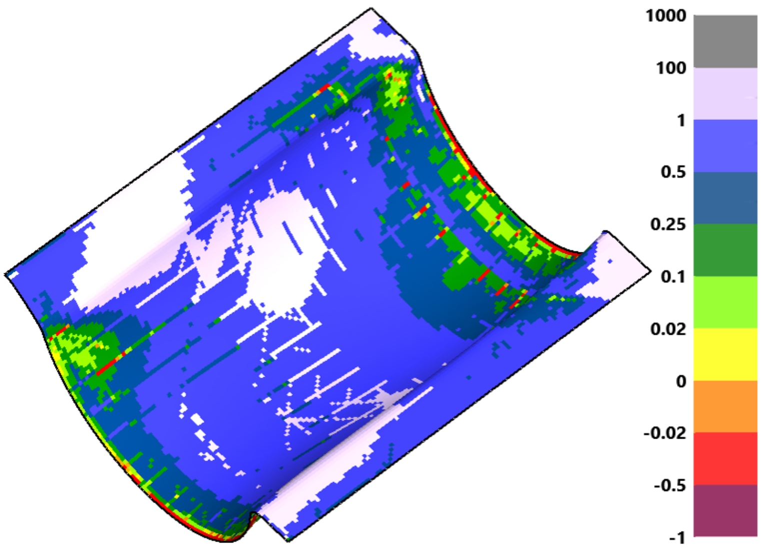

Figure 18. Strength margin analysis updated with fiber deviation and laps/gaps.

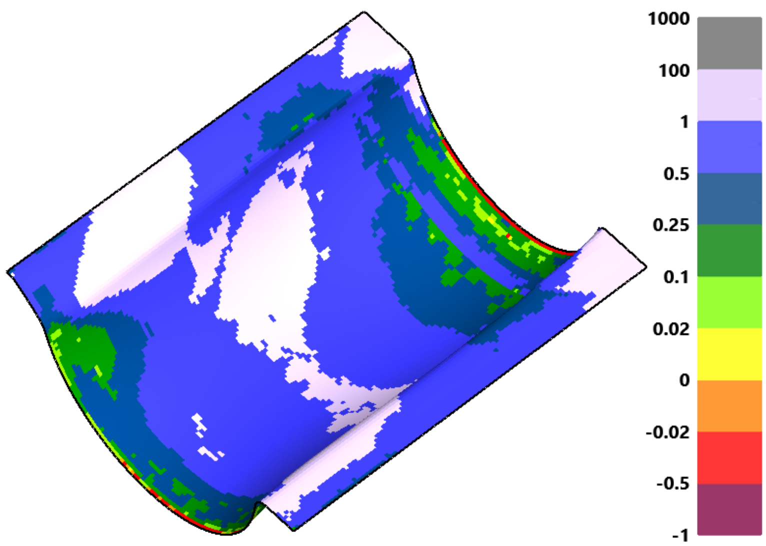

Figure 19. Margins with fiber deviation and laps/gaps, with FEA iteration.

DESIGN UPDATE

The margin plot shown in the previous section indicates that the design must be updated to satisfy the strength requirements. The analysis progression discussed previously indicates that the negative margins were due to fiber angle deviation between the assumed rosette direction and the as-manufactured fiber directions predicted by VCP, and were not caused by the presence of laps and gaps. Sometimes, negative margins due to fiber angle deviation can be resolved by simply rotating the offending plies to compensate for the deviation. This is the preferred solution because it does not increase the weight of the structure. For the IFS however, rotating the plies is not a viable solution due to the symmetry of the structure and the locations of the negative margins. Rotating the 0° and 90° plies is not viable because the symmetry of the structure would cause undesirable deviation elsewhere. Rotating the 45° plies was found to have little impact on the negative margins because these plies are not critical in the location of the negative margins.

For these reasons, the chosen solution was to add a ply to the areas with negative margin. Adding a 90° ply to both ends of the structure was found to provide the most improvement to the negative margins. The location of the added plies is shown in Figure 20. The addition of these plies provided positive margins in the entirety of the IFS, as shown in Figure 21.

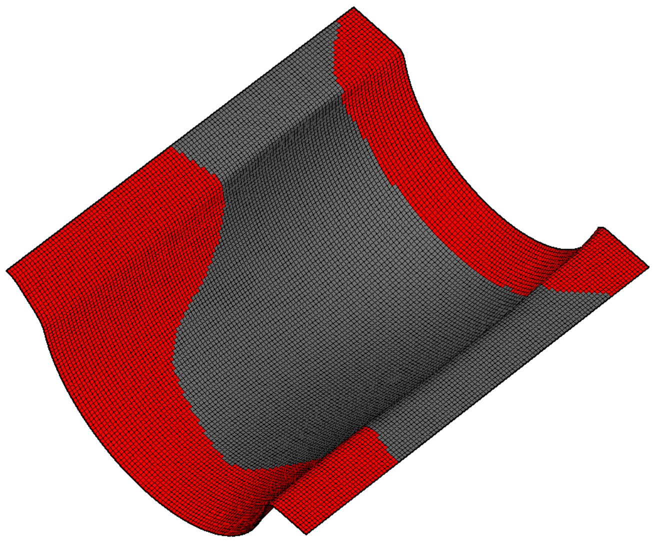

Figure 20. Locations of added plies.

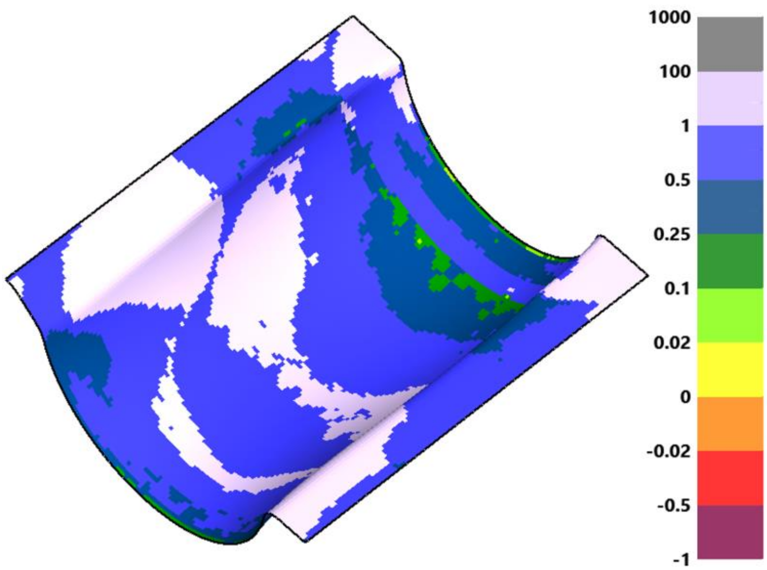

Figure 21. Final strength margins.

CONCLUSIONS

A process has been demonstrated to synchronize strength analysis performed in HyperSizer with AFP manufacturing data produced by VCP. The mapping of fiber directions and laps/gaps helps to align the analysis with the manufacturing process. This enables design processes to be less reliant on blanket specifications that manufacturing engineers are often required to follow. These specifications are usually intended to be all-encompassing to prevent structural failure due to discrepancies between analysis and manufacturing. As a result, the design tends to be conservative and thus potentially increases the weight of the structure as well as increases time spent designing the AFP tow paths. The presented mapping and analysis process realizes the integration of manufacturing considerations in the laminate design process, thus reducing design time and saving weight.

REFERENCES

1. HyperSizer, Software Package, Ver. 7.3.60, Collier Research Corporation, Newport News, VA, 2018.
2. Tsai, S., and Wu, E. 1971. "A General Theory of Strength for Anisotropic Materials," *Journal of Composite Materials*. 58-80.
3. Tsai, S., and Hahn, H. 1980. *Introduction to Composite Materials*. Lancaster: Technomic Publishing Company.
4. CATIA, Software Package, Ver. 5, Dassault Systems, Velizey, France, 2018.
5. Noevere, A.T. and Collier, C.S. 2018. "Mapping Manufacturing Data for Stress Analysis of Automated Fiber Placement Structures." *Structures, Structural Dynamics, and Materials Conference*.